Kim *et al. EURASIP Journal on Wireless Communications and Networking* (2016) 2016:177
DOI 10.1186/s13638-016-0677-2

EURASIP Journal on Wireless Communications and Networking

RESEARCH Open Access

One-shot cooperative beamforming for downlink multicell systems

Doohee Kim[1], Illsoo Sohn[2] and Kwang Bok Lee[1*]

Abstract

We propose a one-shot (non-iterative) cooperative beamforming scheme for downlink multicell systems. Unlike previous non-iterative beamforming schemes, the proposed cooperative beamforming strives to balance maximizing the desired signal power while minimizing the generated interference power to neighbors by maximizing the network-wide average sum rate. Based on the average sum rate analysis, we derive what we term a "global selfishness" that steers the egoistic-altruistic balance of the network to maximize average sum rate. The global selfishness enables an autonomous decision on the cooperative beamforming vector in each cell. The main advantage of our approach is that cooperative beamforming solutions are analytically derived not only for an ideal two-cell network scenario but also for a practical three-sectored cellular network scenario. The simulation results verify that the proposed one-shot cooperative beamforming outperforms other conventional non-iterative schemes especially in interference-limited regions, which implies that it is very effective for performance improvement of edge users.

Keywords: One-shot beamforming, Multicell, Interference management

1 Introduction

Intercell interference (ICI) has been one of the most dominating factors that limits the performance of cellular systems. The sum rate performance is significantly degraded by ICI particularly when a small number of frequency reuse factor is adopted in the network [1, 2]. Thus, there have been seamless efforts to efficiently manage ICI by introducing cooperative beamforming among cells. A well-known example of this effort is the coordinated multi-point (CoMP) technique, which has been rigorously developed for commercial third-generation partnership project long-term evolution (3GPP-LTE) systems [3, 4]. The main hurdle for the network-wide sum rate maximization is in its mathematical intractability. It is very difficult to determine the cooperative beamforming vectors that maximize the desired signal power of one cell while minimizing the generated interference to other cells, as they are all coupled in terms of the sum rate. For the multiple transmit antennas at base station (BS), maximizing the the sum rate is proven to be NP-hard in [5]. Therefore, some alternative approaches have been proposed in the literature [6–20].

The approaches in [6–14] are based on a well-known game theory. The characterizations of achievable rate region and existence of a unique Nash equilibrium have been provided in [6]. Cooperative beamforming vectors are determined by utilizing the two extreme solutions as the basis, i.e., egoistic beamforming and altruistic beamforming. A simple linear-type combination of egoistic beamforming and altruistic beamforming has been shown to achieve Pareto optimality in multiple-input single-output (MISO) systems [7]. The extension to a general K-user case has been derived in [8, 9]. For the case when the partial CSI is available at the transmitter, Pareto optimality of MISO system has been shown in [10]. The analysis based on competitive market, called Walrasian market, has been studied in [11]. The ICI links and beamforming vectors are considered consumers and goods, respectively. Then, the arbitrator coordinates the transmission strategies for achieving the Pareto optimal Walrasian equilibrium. In [12], a beamforming scheme that uses the generated interference level as a bargaining value has been proposed, where both of instantaneous and statistical CSI are considered. The non-strict Pareto boundary of two-user MIMO scenario has been

*Correspondence: klee@snu.ac.kr
[1] Department of Electrical and Computer Engineering, INMC, Seoul National University, Gwanak-ro, 08826 Seoul, South Korea
Full list of author information is available at the end of the article

derived in [13]. It has solved a non-convex problem with rate constraints and an extended K-user MIMO system. The second-order cone programming (SOCP) convex problem has been solved for Pareto optimal points in the achievable rate region of MISO systems in [14]. It has been shown to achieved Pareto optimality in M cell MISO systems. Unfortunately, the aforementioned cooperative beamformings require iterative update procedures to compute cooperative beamforming vectors. Each BS has to recompute new beamforming vectors whenever channel conditions are changed. Thus, this type of approaches typically leads to high computational burden for practical implementations.

For computationally efficient solutions, the approaches in [15–20] propose non-iterative beamforming schemes. To this end, instead of directly maximizing the sum rate, they aim to define a new metric that considers both desired signal power and generating interference power, maximizing the new metric. In [15] and [16], a new metric is defined as the desired signal power and the generated interference power to neighboring cells plus noise power ratio (SGINR). Then, the cooperative beamforming vector in each cell is individually determined to maximize the SGINR. The SGINR-based cooperative beamforming maximizes the desired signal power and minimizes the generated interference power to neighbors simultaneously, which increases the network-wide sum rate. In an ideal two-cell network scenario, the SGINR-based cooperative beamforming has been shown to achieve near optimal performance that maximizes the network-wide sum rate. For general n-cell cases, the optimality of the SGINR-based cooperative beamforming has not been proved, but the main idea can be generalized by assuming high signal-to-interference-plus-noise ratio (SINR) at all links [16]. In [17–19], similar beamforming schemes have been proposed, which maximize virtual SINR. For an ideal two-cell network scenario, it has been shown that linear-type combination of egoistic beamforming and altruistic beamforming achieves Pareto optimality. In [20], the distributed beamforming scheme that maximizes virtual SINR has been proposed. It has studied reciprocity of the uplink and downlink channels in MISO interference channel to propose the distributed beamforming scheme. The closed-form beamforming solution for K-user MISO interference channel has been derived with some assumptions while conventional virtual SINR beamforming solutions have been derived for a two-user scenario. Although the aforementioned non-iterative beamformings in [15–20] maximize SGINR or virtual SINR metric, it is not guaranteed that they can maximize the network-wide sum rate in practical cellular networks.

In this paper, we propose a one-shot cooperative beamforming scheme that does not require iterative computations to determine cooperative beamforming vectors. Unlike previous works that focus on maximizing the instantaneous sum rate or virtual SINR, the proposed one-shot cooperative beamforming instead focuses on maximizing the average sum rate. This enables autonomous decision-making in each cell according to the predetermined metric, called "global selfishness." Global selfishness implies how much each cell in the network may operate selfishly or altruistically to maximize the network-wide sum rate. This can be computed by analyzing the long-term characteristic of the network, i.e., average sum rate. The main advantage of our approach is that we can derive the cooperative beamforming vectors for a practical three-sectored cellular network scenario as well as an ideal two-cell network scenario, which can be achieved in proposed one-shot beamforming approaches without high SINR assumption unlike the conventional non-iterative beamforming approaches. Based on this, we provide a very useful beamforming strategy for practical cellular systems.

Our main contributions are summarized as follows:

- Non-iterative beamforming scheme: We propose a non-iterative beamforming scheme by using global selfishness. According to statistical channel conditions and given global selfishness, each BS dynamically determines whether to behave selfishly or altruistically to maximize network-wide sum rate. Unlike the conventional iterative beamforming schemes, the proposed beamforming scheme requires much less computational complexity.
- Closed-form solution for network-wide sum rate maximization: We derive a closed-form expression of the approximate network-wide sum rate. Based on the closed-form expression, we determine the optimal value of global selfishness that maximizes network-wide sum rate. Considering that previous non-iterative beamforming schemes aim to maximize alternate performance metric, e.g., virtual SINR, our approach directly tackles network-wide sum rate.
- Expanding to general multicell systems: The proposed beamforming scheme can be easily extended to three-sectored cellular network scenario, which is the most typical structure in recent wireless systems. The conventional schemes maximize the alternate performance metric, e.g., sum of the virtual SINR metric, instead of sum rate metric. Moreover, the conventional schemes assume high SINR, which is not valid for cell edge regions. For these reasons, the performance gap between aiming to maximize alternate performance metric and aiming to maximize sum rate metric becomes larger in general three-sectored cellular cases. Our approach easily enables this extension because the proposed scheme

focuses on directly maximizing network-wide sum rate and all the SINR regions.

The rest of this paper is organized as follows. Section 2 describes the system model. In Section 3, we explain the previous cooperative beamforming schemes. In Section 4, we develop a beamforming scheme by deriving a simple metric for the sum rate. In Section 5, we determine the global selfishness for ideal two-cell and practical three-sectored networks. Moreover, we expand our scheme for general N_t transmit antennas systems. Numerical results are presented in Section 6, and conclusions are drawn in Section 7.

Notations: The boldface small letters denote vectors. $|\cdot|$ denotes a norm, $\mathbb{P}(\cdot)$ denotes a probability, and $\mathbb{E}[\cdot]$ denotes an expectation.

2 System model

We consider a downlink cellular system comprised of M cells. We assume that single mobile station (MS) in each cell is already selected to be served by scheduler. Each BS is equipped with N_t antennas and the MS has a single antenna. As depicted in Fig. 1, it is an example of $M = 3$ cellular network system. The received signal vector $\mathbf{y}_i$ at the MS in the ith cell can be expressed as

$$\mathbf{y}_i = \sqrt{\rho_i}\mathbf{h}_{ii}\mathbf{w}_i\mathbf{x}_i + \sum_{j=1,j\neq i}^{M} \sqrt{\rho_{ji}}\mathbf{h}_{ji}\mathbf{w}_j\mathbf{x}_j + \mathbf{n}_i, \tag{1}$$

where $\mathbf{h}_{ji}$ denotes $1 \times N_t$ channel vector between BS in the jth cell and the MS in the ith cell, $\mathbf{w}_i$ denotes $N_t \times 1$ corresponding beamforming vector at the BS in the ith cell, and it is normalized, i.e., $||\mathbf{w}_i||^2 = 1$. $\mathbf{x}_i$ is the signal transmitted from the ith BS to the ith MS. We assume that the elements of $\mathbf{h}_{ji}$ follow independent and identically distributed complex Gaussian distribution with zero mean and unit variance. In addition, $\mathbf{n}_i$ denotes the additive white Gaussian noise (AWGN) at the ith MS with unit variance, ρ_i denotes the average signal-to-noise ratio (SNR) of the MS in the ith cell, and ρ_{ji} is the average interference-to-noise ratio (INR) for the interference that the BS in the jth cell causes to the MS in the ith cell. The received SINR γ_i of the MS in the ith cell can be computed from Eq. (1) as

$$\gamma_i = \frac{\rho_i|\mathbf{h}_{ii}\mathbf{w}_i|^2}{1 + \sum\limits_{j=1,j\neq i}^{M} \rho_{ji}|\mathbf{h}_{ji}\mathbf{w}_j|^2}. \tag{2}$$

From Eq. (2), the network-wide sum rate of all cells $\mathcal{R}$ is given as

$$\mathcal{R} = \sum_{i=1}^{M} \log_2(1+\gamma_i). \tag{3}$$

3 Previous cooperative beamforming schemes

In this section, we review cooperative beamforming schemes that have been studied recently: the iterative

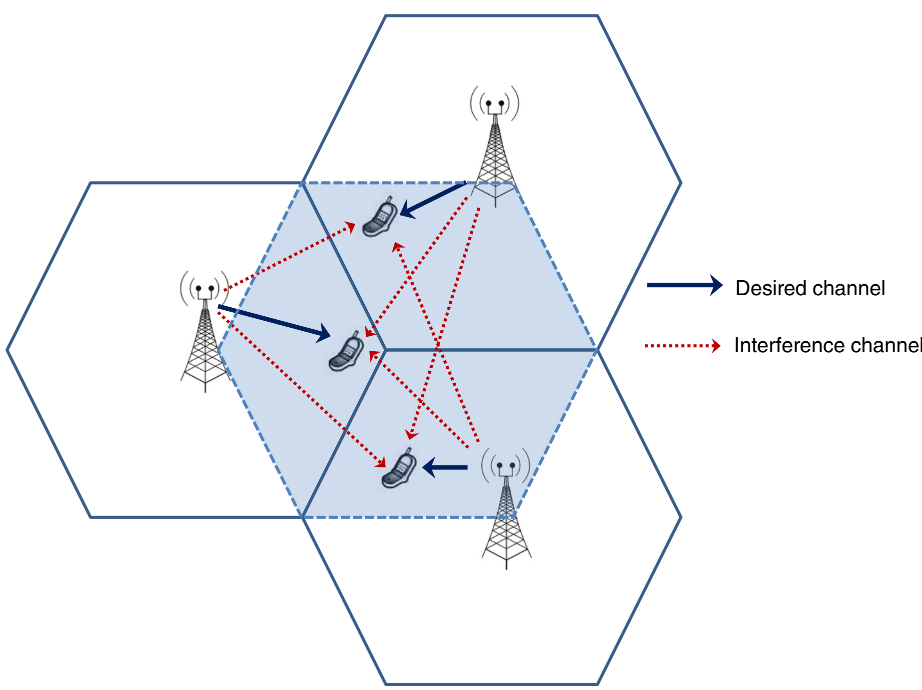

Fig. 1 $M = 3$ cellular network for multicell system

Pareto optimality beamforming [7] and the virtual SINR maximizing beamforming [17].

3.1 Iterative Pareto optimality beamforming

The iterative Pareto optimality beamforming scheme consider the special case of two BSs and two MSs. It is shown that the linear combination of the zero-forcing (ZF) beamforming and the maximum-ratio transmission (MRT) beamforming with real-valued coefficients achieves Pareto optimality in MISO systems. The beamforming vector at the BS in the kth cell that is achievable Pareto optimality can be expressed as

$$\mathbf{w}_k(\alpha_k) = \frac{\alpha_k \mathbf{w}_k^{\mathrm{MRT}} + (1-\alpha_k)\mathbf{w}_k^{\mathrm{ZF}}}{||\alpha_k \mathbf{w}_k^{\mathrm{MRT}} + (1-\alpha_k)\mathbf{w}_k^{\mathrm{ZF}}||}, \quad k = 1, 2. \quad (4)$$

α_k is set some real-valued parameters, $0 \leq \alpha_k \leq 1$. And $\mathbf{w}_k^{\mathrm{ZF}}$ and $\mathbf{w}_k^{\mathrm{MRT}}$ represent ZF beamforming vector and MRT beamforming vector of the BS in the kth cell, respectively. The Pareto optimality beamforming achieves optimal Pareto boundary with proper α_1 and α_2. However, it leads high computational burden for practical implementation due to iterative processes for determining proper α_1 and α_2. Moreover, its application is limited to systems where there exists two BSs and two MSs.

3.2 Virtual SINR maximizing beamforming

In virtual SINR maximizing beamforming scheme, virtual SINR metric is modified from SINR and defined as the desired signal power and the generated interference power to neighboring cells plus noise power ratio. It can be expressed as

$$\gamma_k^{\mathrm{vs}} = \frac{\rho_k |\mathbf{h}_{kk}\mathbf{w}_k|^2}{\sigma^2 + \sum_{j \neq k}^{M} \rho_{kj} |\mathbf{h}_{kj}\mathbf{w}_k|^2}, \quad (5)$$

where σ^2 denotes the noise power. Virtual SINR maximizing beamforming scheme proposes that each BS solve a virtual SINR maximization problem and it can be stated as

$$\mathbf{w}_k = \underset{||\mathbf{w}||^2=1}{\arg\max} \frac{\rho_k |\mathbf{h}_{kk}\mathbf{w}_k|^2}{\sigma^2 + \sum_{j \neq k}^{M} \rho_{kj} |\mathbf{h}_{kj}\mathbf{w}_k|^2}. \quad (6)$$

In a scenario where there exists two BSs and two MSs, the virtual SINR maximizing beamforming scheme has been shown to achieve near optimal performance in terms of network-wide sum rate. The virtual SINR beamforming scheme can be extended to general n-cell cases by assuming high SINR, i.e., ignoring interference and noise power. However, the generalized scheme does not guarantee optimal solutions. Moreover, this approach becomes inefficient especially for cell edge region where MSs typically experience low SINR.

4 Proposed one-shot cooperative beamforming

In this section, we propose a new one-shot cooperative beamforming that operates in a non-iterative manner. The proposed one-shot cooperative beamforming focuses on maximizing the average sum rate. At the cost of averaging out local interactions of the network, we can achieve the network-wide balance between egoism and altruism for cooperative beamforming vector computations. The derived metric, global selfishness, significantly relieves the computational burden by providing a simple decision rule for computing cooperative vectors in each cell. In Fig. 2, we illustrate the detailed procedure of the proposed beamforming scheme. The proposed beamforming

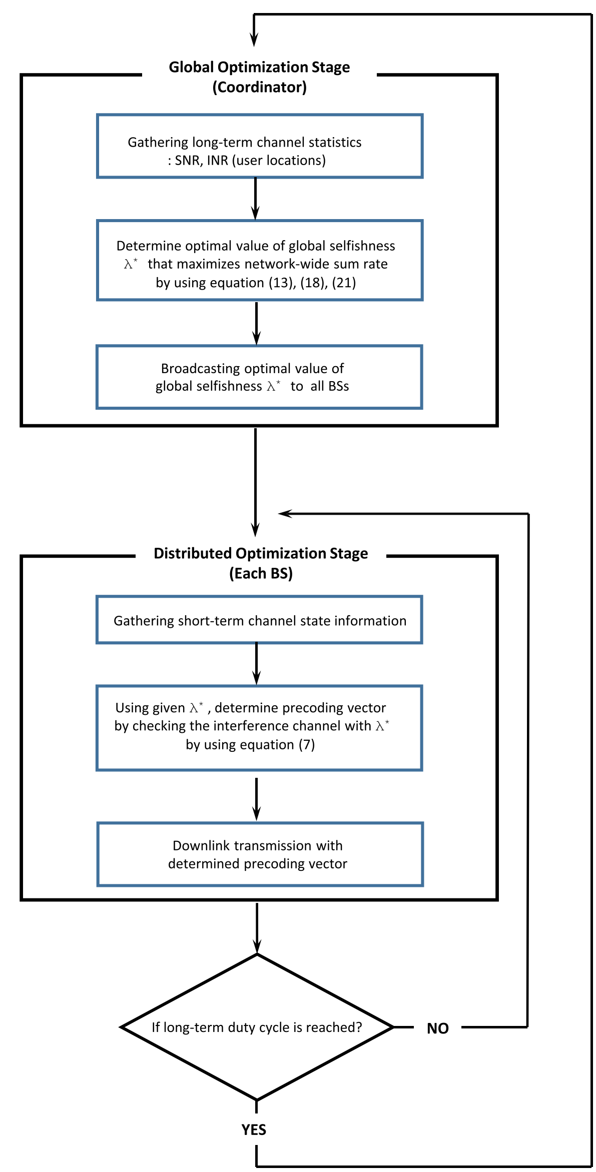

Fig. 2 Framework of the proposed beamforming scheme

scheme consists of two stages, i.e., global optimization stage and distributed optimization stage. A network coordinator in the global optimization stage gathers long-term channel statistics, i.e., SNR and INR are influenced by location of users and transmit power. On the basis of gathered long-term information, the network coordinator determines the optimal value of global selfishness $\lambda^\star$ that maximizes network-wide sum rate. The network-wide sum rate analysis and the detailed derivation of the decision metric will be described in the following section. Then, the network coordinator broadcasts the optimal value of global selfishness $\lambda^\star$ to all BSs. Each BS in the distributed optimization stage gathers short-term CSI and determines precoding vectors by checking the CSI of interference channel with $\lambda^\star$. Then, each BS transmits signals for users with determined precoding vector. During normal downlink transmission, each BS operates in a distributed optimization stage. At the end of long-term duty cycle, the updating process of global selfishness is initiated in the global optimization stage.

The global selfishness can be interpreted as the amount that each cell can behave selfishly or altruistically to maximize the network-wide sum rate. The optimal value of the global selfishness $\lambda^\star$ is precomputed and shared as a network policy. Once BSs share the optimal value of global selfishness $\lambda^\star$ that is computed by the network coordinator in the global optimization stage, each BS simply computes precoding vector with $\lambda^\star$ in the distributed optimization stage and the required CSI for beamforming is same as distributed beamforming schemes. Since the updating process of global selfishness requires long-term duty cycle, amount of sharing information among BSs becomes minimal as in distributed beamforming schemes. Regarding computational complexity, the proposed scheme can reduce computational burden compared to centralized beamforming schemes. The computational burden in the global optimization stage has less influence on the complexity of the whole system since the updating process of global selfishness requires a long-term duty cycle. In this sense, the proposed beamforming scheme works in semi-distributed manner. Each cell behaves either selfishly or altruistically according to the statistical channel conditions and given $\lambda^\star$. Specifically, the ith cell determines whether its interference links to neighboring cells are dominant or not by checking the channel gains of the interference links with $\lambda^\star$ as $\Phi_i = \{j| \, \|\mathbf{h}_{ij}\|^2 \geq \lambda^\star\}$, where Φ_i denotes the set of dominant interference links of the ith cell. The beamforming vector is then computed to nullify the dominant interference links as

$$\left|\mathbf{h}_{ij}\mathbf{w}_i\right|^2 = 0, \quad \forall j \in \Phi_i. \tag{7}$$

When $\lambda^\star$ is small, the entire network enters an altruistic mood where each cell tends to determine its cooperative beamforming vector that nullifies interference power to its neighboring cells. In the limit of $\lambda^\star \rightarrow 0$, the proposed beamforming nullifies all the interference links and becomes equivalent to the well-known ZF beamforming. The opposite is true for large $\lambda^\star$, and the proposed beamforming becomes equivalent to the MRT beamforming in the limit of $\lambda^\star \rightarrow \infty$.

Note that the proposed beamforming scheme can reduce computation complexity by using global selfishness. The computation complexity of beamforming scheme mainly comes from computations of precoding vectors. The proposed beamforming scheme requires only a single matrix inversion of precoding vector; however, the conventional iterative beamforming schemes requires dozens of computations for precoding vectors. Therefore, compared to conventional iterative beamforming schemes, the proposed beamforming scheme can significantly reduce the computational burden.

5 Determination of global selfishness λ

In this section, we first describe how to determine the optimal value of global selfishness for an ideal two-cell network scenario. Then, we expend our results to a practical three-sectored cellular network scenario. For easy understanding, we provide derivations assuming two transmit antennas in Sections 5.1 and 5.2. However, our results are not limited to the case. We expand our scheme to arbitrary N_t transmit antennas scenario in Section 5.3.

5.1 Ideal two-cell network scenario

We describe how to determine the optimal value of global selfishness for an ideal two-cell network scenario. There exist four possible cases depending on whether each BS acts in an egoistic or an altruistic way. Those cases and corresponding probabilities are tabulated in Table 1, where ψ is defined as $\psi = \mathbb{P}\left(||\mathbf{h}_{ji}||^2 > \lambda\right)$ and $\bar{\psi} = 1 - \psi$. Case 1 implies that all BSs operate selfishly where no BS nullifies interference links. In case 2 and case 3, one BS nullifies its generated interference link, and the other BS operates selfishly. Case 4 implies that all BSs nullify the generated interference link and all MSs whose received

Table 1 BSs actions and corresponding probabilities

Case number	BS_1 action	BS_2 action	Probability
Case 1	Egoistic	Egoistic	$\bar{\psi}^2$
Case 2	Egoistic	Altruistic	$\bar{\psi}\psi$
Case 3	Altruistic	Egoistic	$\bar{\psi}\psi$
Case 4	Altruistic	Altruistic	ψ^2

interference link are nullified. Then, for further derivations, we define random variable $\Gamma_i^{(e_i,a_i)}$ indicates SINR of the MS in the ith cell where the ith BS nullifies e_i generated interference links to neighboring cells and a_i received interference links of the MS in the ith cell are nullified by the neighboring BSs. Then, we can expressed $\Gamma_i^{(e_i,a_i)}$ by using ([21], Lemma 2) as

$$\Gamma_i^{(e_i,a_i)} = 1 + \frac{\rho_i \chi^2_{2(N_t-e_i)}}{1+\sum\limits_{j\in\Omega_i} \rho_{ji}\chi_2^2}, \tag{8}$$

where Ω_i denotes the set of neighboring cells of ith cell except the number of a_i BSs that nullify the generated interference links to the MS in the ith cell. χ_n^2 denotes the Chi-square distribution random variable with n degrees of freedom. Then, considering the four possible cases and given ψ, we derive $\mathcal{R}(\psi)$ the sum rate function of ψ from Eq. (3) using Eq. (8) as

$$\begin{aligned}\mathcal{R}(\psi) =& \bar{\psi}^2 \log_2\left(\Gamma_1^{(0,0)}\Gamma_2^{(0,0)}\right) + \psi^2\log_2\left(\Gamma_1^{(1,1)}\Gamma_2^{(1,1)}\right)\\ &+ \psi\bar{\psi}\left(\log_2\left(\Gamma_1^{(0,1)}\Gamma_2^{(1,0)}\right) + \log_2\left(\Gamma_1^{(1,0)}\Gamma_2^{(0,1)}\right)\right)\\ =& \bar{\psi}^2\log_2\left(\Pi_{(0,0)}^{(0,0)}\right) + \psi^2\log_2\left(\Pi_{(1,1)}^{(1,1)}\right) + \psi\bar{\psi}\log_2\left(\Pi_{(1,0)}^{(0,1)}\Pi_{(0,1)}^{(1,0)}\right),\end{aligned} \tag{9}$$

where $\Pi_{(a_1,a_2)}^{(e_1,e_2)}$ represents the product of $\Gamma_i^{(e_i,a_i)}$ is defined as

$$\Pi_{(a_1,a_2,..,a_n)}^{(e_1,e_2,..,e_n)} = \Gamma_1^{(e_1,a_1)}\Gamma_2^{(e_2,a_2)} \times \cdots \times \Gamma_n^{(e_n,a_n)}. \tag{10}$$

For sum rate analysis, we derive the expected sum rate and its upper bound is denoted as $\mathcal{R}^{\mathrm{U}}(\psi)$. Then, it can be expressed as

$$\begin{aligned}\mathbb{E}[\mathcal{R}(\psi)] =& \bar{\psi}^2\mathbb{E}\left[\log_2\left(\Pi_{(0,0)}^{(0,0)}\right)\right] + \psi^2\mathbb{E}\left[\log_2\left(\Pi_{(1,1)}^{(1,1)}\right)\right]\\ &+ \psi\bar{\psi}\mathbb{E}\left[\log_2\left(\Pi_{(1,0)}^{(0,1)}\Pi_{(0,1)}^{(1,0)}\right)\right]\\ \le& \bar{\psi}^2\log_2\left(\mathbb{E}\left[\Pi_{(0,0)}^{(0,0)}\right]\right) + \psi^2\log_2\left(\mathbb{E}\left[\Pi_{(1,1)}^{(1,1)}\right]\right)\\ &+ \psi\bar{\psi}\log_2\left(\left(\mathbb{E}\left[\Pi_{(1,0)}^{(0,1)}\right]\right)\left(\mathbb{E}\left[\Pi_{(0,1)}^{(1,0)}\right]\right)\right)\\ \equiv& \mathcal{R}^{\mathrm{U}}(\psi),\end{aligned} \tag{11}$$

where the inequality follows from Jensen's inequality. $\Gamma_1^{(e_1,a_1)}$ and $\Gamma_2^{(e_2,a_2)}$ are independent, then the expectation of $\Pi_{(a_1,a_2)}^{(e_1,e_2)}$ can be expressed as

$$\bar{\Pi}_{(a_1,a_2)}^{(e_1,e_2)} = \mathbb{E}\left[\Pi_{(a_1,a_2)}^{(e_1,e_2)}\right] = \mathbb{E}\left[\Gamma_1^{(e_1,a_1)}\right]\mathbb{E}\left[\Gamma_2^{(e_2,a_2)}\right]. \tag{12}$$

We derive the details of $\mathbb{E}\left[\Gamma_i^{(e_i,a_i)}\right]$ of (12) in Appendix A. Then, $\mathcal{R}^{\mathrm{U}}(\psi)$ can be expressed as

$$\begin{aligned}\mathcal{R}^{\mathrm{U}}(\psi) =& \bar{\psi}^2\log_2\left(\bar{\Pi}_{(0,0)}^{(0,0)}\right) + \psi^2\log_2\left(\bar{\Pi}_{(1,1)}^{(1,1)}\right) + \psi\bar{\psi}\log_2\left(\bar{\Pi}_{(1,0)}^{(0,1)}\bar{\Pi}_{(0,1)}^{(1,0)}\right)\\ =& a\psi^2 + b\psi + c,\end{aligned}$$

and

$$a \equiv \log_2\left(\frac{\bar{\Pi}_{(0,0)}^{(0,0)}\bar{\Pi}_{(1,1)}^{(1,1)}}{\bar{\Pi}_{(1,0)}^{(0,1)}\bar{\Pi}_{(0,1)}^{(1,0)}}\right), b \equiv \log_2\left(\frac{\bar{\Pi}_{(1,0)}^{(0,1)}\bar{\Pi}_{(0,1)}^{(1,0)}}{\left(\bar{\Pi}_{(0,0)}^{(0,0)}\right)^2}\right), c \equiv \log_2\left(\bar{\Pi}_{(0,0)}^{(0,0)}\right). \tag{13}$$

Using the closed-form expression of $\mathcal{R}^{\mathrm{U}}(\psi)$ in Eq. (13), we determine the optimal value $\psi^\star$ that maximizes $\mathcal{R}^{\mathrm{U}}(\psi)$ as

$$\psi^\star = \arg\max_{\psi} \mathcal{R}^{\mathrm{U}}(\psi). \tag{14}$$

Note that $\mathcal{R}^{\mathrm{U}}(\psi)$ is a quadratic function of ψ. We first consider that $\mathcal{R}^{\mathrm{U}}(\psi)$ is a concave function ($a < 0$). The point of pole ψ^D becomes the optimal point of ψ if ψ^D is located in [0,1]. If ψ^D is less than 0 or greater than 1, the optimal value of ψ is 0 or 1, respectively. Next, we consider that $\mathcal{R}^{\mathrm{U}}(\psi)$ is a convex function ($a > 0$). Either 0 or 1, i.e., whichever is closer to ψ^D, becomes the optimal $\psi^\star$. In short, $\psi^\star$ is determined as

$$\begin{aligned}&\text{(i) } a < 0, \quad \psi^\star = \begin{cases} 0 & \text{if} \quad \psi^D < 0 \\ \psi^D & \text{if} \quad 0 \le \psi^D \le 1 \\ 1 & \text{if} \quad 1 < \psi^D \end{cases}\\ &\text{(ii) } a > 0, \quad \psi^\star = \begin{cases} 0 & \text{if} \quad \left|\psi^D\right| > \left|\psi^D - 1\right| \\ 1 & \text{if} \quad \left|\psi^D\right| \le \left|\psi^D - 1\right|, \end{cases}\\ &\quad\text{where} \quad \psi^D = -b/2a, \ \text{s.t.} \left[\frac{\partial\mathcal{R}^{\mathrm{U}}(\psi)}{\partial\psi}\right]_{\psi=\psi^D} = 0.\end{aligned} \tag{15}$$

Furthermore, we can determine the optimal value of the global selfishness $\lambda^\star$ from $\psi^\star$, since $||\mathbf{h}_{ji}||^2$ has a Gamma(N_t,2) distribution and there is one-to-one correspondence between ψ and λ. The value of $\lambda^\star$ is computed from $\psi^\star$ as

$$\lambda^\star = F^{-1}(1-\psi^\star; N_t, 2), \tag{16}$$

where $F(x; N_t, 2)$ denotes the cumulative distribution function (cdf) of Gamma(N_t,2) and $F^{-1}(\cdot)$ denotes the inverse function of cdf. Thus, $\lambda^\star$ can be uniquely determined with $\psi^\star$.

The principal advantage of the proposed one-shot cooperative beamforming is that it requires much less computational complexity; it only requires a simple comparison of a channel with the given $\lambda^\star$. Since the computational complexity of scheme mainly comes from computations of the precoding vectors, we compare the computational complexity in terms of the required number of computations for precoding vectors. The proposed scheme requires only a single computation of precoding vector, however, the conventional iterative beamforming schemes in [7–12, 14] require dozens of computations for precoding vectors, for example, the iterative scheme in [7] requires about 30 repeats of precoding vector computations.

5.2 Practical three-sectored cellular network scenario

For practical applications of the proposed one-shot beamforming scheme, we extend our results to a three-sectored cellular network scenario, which is the most typical structure in recent wireless systems. Note that the conventional approaches to non-iterative beamforming in [15–20] fail to provide analytic beamforming solution for $M > 2$ cases, without assuming high SINR, which is obviously not valid for cell edge regions. Moreover, the conventional approaches maximize sum of the V-SINR metric instead of sum rate metric and the gap between sum of V-SINR metric and sum rate metric becomes larger in general $M > 2$ cases. Whereas our approach easily enables this extension because the proposed scheme focuses on average sum rate and all the SINR regions, which can be analyzed as follows. For easy understanding, we provide derivations assuming two transmit antennas in the following and BS_i nullifies the most dominant one interference link of Φ_i. However, our results are not limited to the case. In this scenario, each BS has three different actions. Taking BS_1 as an example, those cases and corresponding probabilities are tabulated in Table 2. Since interference channels are independent, BS_1 has same probability for each altruistic action for MS_2 and MS_3. Therefore, there are a total of $3^3 = 27$ different cases for three-sectored networks. Then, $\mathcal{R}(\psi)$ from (3) can be expressed as

$$\begin{aligned}
&\mathcal{R}(\psi)\\
&=\left(\frac{1}{2}\psi\right)^3\log_2\!\left(\Pi^{(1,1,1)}_{(1,1,1)}\Pi^{(1,1,1)}_{(1,1,1)}\Pi^{(1,1,1)}_{(2,1,0)}\Pi^{(1,1,1)}_{(2,0,1)}\Pi^{(1,1,1)}_{(1,2,0)}\Pi^{(1,1,1)}_{(1,0,2)}\Pi^{(1,1,1)}_{(0,2,1)}\Pi^{(1,1,1)}_{(0,1,2)}\right)\\
&\quad+\left(\frac{1}{2}\psi\right)^2\bar{\psi}\log_2\Big(\Pi^{(1,1,0)}_{(1,1,0)}\Pi^{(1,1,0)}_{(0,1,1)}\Pi^{(1,1,0)}_{(1,0,1)}\Pi^{(1,1,0)}_{(0,0,2)}\Pi^{(1,0,1)}_{(1,1,0)}\Pi^{(1,0,1)}_{(0,1,1)}\times\\
&\qquad\qquad\Pi^{(1,0,1)}_{(1,0,1)}\Pi^{(1,0,1)}_{(0,2,0)}\Pi^{(0,1,1)}_{(1,1,0)}\Pi^{(0,1,1)}_{(1,0,1)}\Pi^{(0,1,1)}_{(0,1,1)}\Pi^{(0,1,1)}_{(2,0,0)}\Big)\\
&\quad+\left(\frac{1}{2}\psi\right)\bar{\psi}^2\log_2\left(\Pi^{(1,0,0)}_{(0,1,0)}\Pi^{(1,0,0)}_{(0,0,1)}\Pi^{(0,1,0)}_{(1,0,0)}\Pi^{(0,1,0)}_{(0,0,1)}\Pi^{(0,0,1)}_{(1,0,0)}\Pi^{(0,0,1)}_{(0,1,0)}\right)\\
&\quad+\bar{\psi}^3\log_2\left(\Pi^{(0,0,0)}_{(0,0,0)}\right).
\end{aligned}\tag{17}$$

Table 2 BS_1 actions and corresponding probabilities in three-sectored cellular network

Case number	BS_1 action	Probability
Case 1	Egoistic	$\bar{\psi}$
Case 2	Altruistic for MS_2	$(1/2)\psi$
Case 3	Altruistic for MS_3	$(1/2)\psi$

Then, we derive the expected sum rate and its upper bound for sum rate analysis in the same way of (11). The expectation of $\Gamma_i^{(e_i,a_i)}$ for three-sectored cellular scenario is derived in Appendix B. Since $\Gamma_1^{(e_1,a_1)}$, $\Gamma_2^{(e_2,a_2)}$, and $\Gamma_3^{(e_3,a_3)}$ are independent, we can easily calculate $\bar{\Pi}^{(e_1,e_2,e_3)}_{(a_1,a_2,a_3)}$. Therefore, $\mathcal{R}^{\mathrm{U}}(\psi)$ can be expressed as

$$\begin{aligned}
&\mathbb{E}[\,\mathcal{R}(\psi)]\\
&\le\left(\frac{1}{2}\psi\right)^3\log_2\!\left(\bar{\Pi}^{(1,1,1)}_{(1,1,1)}\bar{\Pi}^{(1,1,1)}_{(1,1,1)}\bar{\Pi}^{(1,1,1)}_{(2,1,0)}\bar{\Pi}^{(1,1,1)}_{(2,0,1)}\bar{\Pi}^{(1,1,1)}_{(1,2,0)}\bar{\Pi}^{(1,1,1)}_{(1,0,2)}\bar{\Pi}^{(1,1,1)}_{(0,2,1)}\bar{\Pi}^{(1,1,1)}_{(0,1,2)}\right)\\
&\quad+\left(\frac{1}{2}\psi\right)^2\bar{\psi}\log_2\Big(\bar{\Pi}^{(1,1,0)}_{(1,1,0)}\bar{\Pi}^{(1,1,0)}_{(0,1,1)}\bar{\Pi}^{(1,1,0)}_{(1,0,1)}\bar{\Pi}^{(1,1,0)}_{(0,0,2)}\bar{\Pi}^{(1,0,1)}_{(1,1,0)}\bar{\Pi}^{(1,0,1)}_{(0,1,1)}\times\\
&\qquad\qquad\bar{\Pi}^{(1,0,1)}_{(1,0,1)}\bar{\Pi}^{(1,0,1)}_{(0,2,0)}\bar{\Pi}^{(0,1,1)}_{(1,1,0)}\bar{\Pi}^{(0,1,1)}_{(1,0,1)}\bar{\Pi}^{(0,1,1)}_{(0,1,1)}\bar{\Pi}^{(0,1,1)}_{(2,0,0)}\Big)\\
&\quad+\left(\frac{1}{2}\psi\right)\bar{\psi}^2\log_2\left(\bar{\Pi}^{(1,0,0)}_{(0,1,0)}\bar{\Pi}^{(1,0,0)}_{(0,0,1)}\bar{\Pi}^{(0,1,0)}_{(1,0,0)}\bar{\Pi}^{(0,1,0)}_{(0,0,1)}\bar{\Pi}^{(0,0,1)}_{(1,0,0)}\bar{\Pi}^{(0,0,1)}_{(0,1,0)}\right)\\
&\quad+\bar{\psi}^3\log_2\left(\bar{\Pi}^{(0,0,0)}_{(0,0,0)}\right)\\
&=a\psi^3+b\psi^2+c\psi+d\equiv\mathcal{R}^{\mathrm{U}}(\psi),
\end{aligned}\tag{18}$$

where

$$\begin{aligned}
a\equiv{}&\log_2\Bigg[\left(\bar{\Pi}^{(1,1,1)}_{(1,1,1)}\bar{\Pi}^{(1,1,1)}_{(1,1,1)}\bar{\Pi}^{(1,1,1)}_{(2,1,0)}\bar{\Pi}^{(1,1,1)}_{(2,0,1)}\bar{\Pi}^{(1,1,1)}_{(1,2,0)}\bar{\Pi}^{(1,1,1)}_{(1,0,2)}\bar{\Pi}^{(1,1,1)}_{(0,2,1)}\bar{\Pi}^{(1,1,1)}_{(0,1,2)}\right)^{\frac{1}{8}}\\
&\qquad\times\left(\bar{\Pi}^{(1,0,0)}_{(0,1,0)}\bar{\Pi}^{(1,0,0)}_{(0,0,1)}\bar{\Pi}^{(0,1,0)}_{(1,0,0)}\bar{\Pi}^{(0,1,0)}_{(0,0,1)}\bar{\Pi}^{(0,0,1)}_{(1,0,0)}\bar{\Pi}^{(0,0,1)}_{(0,1,0)}\right)^{\frac{1}{2}}\Bigg]\\
&-\log_2\Bigg[\left(\bar{\Pi}^{(1,1,0)}_{(1,1,0)}\bar{\Pi}^{(1,1,0)}_{(0,1,1)}\bar{\Pi}^{(1,1,0)}_{(1,0,1)}\bar{\Pi}^{(1,1,0)}_{(0,0,2)}\bar{\Pi}^{(1,0,1)}_{(1,1,0)}\bar{\Pi}^{(1,0,1)}_{(0,1,1)}\bar{\Pi}^{(1,0,1)}_{(1,0,1)}\right)^{\frac{1}{4}}\\
&\qquad\times\left(\bar{\Pi}^{(1,0,1)}_{(0,2,0)}\bar{\Pi}^{(0,1,1)}_{(1,1,0)}\bar{\Pi}^{(0,1,1)}_{(1,0,1)}\bar{\Pi}^{(0,1,1)}_{(0,1,1)}\bar{\Pi}^{(0,1,1)}_{(2,0,0)}\right)^{\frac{1}{4}}\left(\bar{\Pi}^{(0,0,0)}_{(0,0,0)}\right)\Bigg],\\
b\equiv{}&\log_2\Bigg[\left(\bar{\Pi}^{(1,1,0)}_{(1,1,0)}\bar{\Pi}^{(1,1,0)}_{(0,1,1)}\bar{\Pi}^{(1,1,0)}_{(1,0,1)}\bar{\Pi}^{(1,1,0)}_{(0,0,2)}\bar{\Pi}^{(1,0,1)}_{(1,1,0)}\bar{\Pi}^{(1,0,1)}_{(0,1,1)}\bar{\Pi}^{(1,0,1)}_{(1,0,1)}\right)^{\frac{1}{4}}\\
&\qquad\times\left(\bar{\Pi}^{(1,0,1)}_{(0,2,0)}\bar{\Pi}^{(0,1,1)}_{(1,1,0)}\bar{\Pi}^{(0,1,1)}_{(1,0,1)}\bar{\Pi}^{(0,1,1)}_{(0,1,1)}\bar{\Pi}^{(0,1,1)}_{(2,0,0)}\right)^{\frac{1}{4}}\left(\bar{\Pi}^{(0,0,0)}_{(0,0,0)}\right)^3\Bigg]\\
&-\log_2\left(\bar{\Pi}^{(1,0,0)}_{(0,1,0)}\bar{\Pi}^{(1,0,0)}_{(0,0,1)}\bar{\Pi}^{(0,1,0)}_{(1,0,0)}\bar{\Pi}^{(0,1,0)}_{(0,0,1)}\bar{\Pi}^{(0,0,1)}_{(1,0,0)}\bar{\Pi}^{(0,0,1)}_{(0,1,0)}\right),\\
c\equiv{}&\log_2\left(\bar{\Pi}^{(1,0,0)}_{(0,1,0)}\bar{\Pi}^{(1,0,0)}_{(0,0,1)}\bar{\Pi}^{(0,1,0)}_{(1,0,0)}\bar{\Pi}^{(0,1,0)}_{(0,0,1)}\bar{\Pi}^{(0,0,1)}_{(1,0,0)}\bar{\Pi}^{(0,0,1)}_{(0,1,0)}\right)^{\frac{1}{2}}\\
&\quad-\log_2\left(\bar{\Pi}^{(0,0,0)}_{(0,0,0)}\right)^3,\\
d\equiv{}&\log_2\left(\bar{\Pi}^{(0,0,0)}_{(0,0,0)}\right).
\end{aligned}$$

We determine the optimal value $\psi^\star$ that maximizes $\mathcal{R}^{\mathrm{U}}(\psi)$ in Eq. (18). Given that $\mathcal{R}^{\mathrm{U}}(\psi)$ is a cubic function of ψ, we consider the cases depending on a sign of a and location of poles ψ^{D1}, ψ^{D2} to determine $\psi^\star$. Considering the cases, $\psi^\star$ is determined as

(i) $a < 0$

$$\psi^\star = \begin{cases} 0 & \text{if} \quad \psi^{D1}, \psi^{D2} > 1 \\ \max\limits_{\psi} \left(\mathcal{R}^{\mathrm{U}}(0), \mathcal{R}^{\mathrm{U}}(1)\right) & \text{if} \quad 0 \leq \psi^{D1} \leq 1 \leq \psi^{D2} \\ 0 & \text{if} \quad \psi^{D1} \leq 0 \leq 1 \leq \psi^{D2} \\ \max\limits_{\psi} (\mathcal{R}^{\mathrm{U}}(0), \mathcal{R}^{\mathrm{U}}(\psi^{D2})) & \text{if} \quad 0 \leq \psi^{D1}, \psi^{D2} \leq 1 \\ \psi^{D2} & \text{if} \quad \psi^{D1} \leq 0 \leq \psi^{D2} \leq 1 \\ 0 & \text{if} \quad \psi^{D1}, \psi^{D2} < 0 \end{cases}$$

(ii) $a > 0$

$$\psi^\star = \begin{cases} 1 & \text{if} \quad \psi^{D1}, \psi^{D2} > 1 \\ \psi^{D1} & \text{if} \quad 0 \leq \psi^{D1} \leq 1 \leq \psi^{D2} \\ 1 & \text{if} \quad \psi^{D1} \leq 0 \leq 1 \leq \psi^{D2} \\ \max\limits_{\psi} \left(\mathcal{R}^{\mathrm{U}}(0), \mathcal{R}^{\mathrm{U}}(\psi^{D1})\right) & \text{if} \quad 0 \leq \psi^{D1}, \psi^{D2} \leq 1 \\ \max\limits_{\psi} (\mathcal{R}^{\mathrm{U}}(0), \mathcal{R}^{\mathrm{U}}(1)) & \text{if} \quad \psi^{D1} \leq 0 \leq \psi^{D2} \leq 1 \\ 1 & \text{if} \quad \psi^{D1}, \psi^{D2} < 0, \end{cases} \tag{19}$$

$$\text{where} \quad \psi^{D1} = (-b - \sqrt{b^2 - 3ac})/3a, \ \psi^{D2} = (-b + \sqrt{b^2 - 3ac})/3a$$
$$\text{s.t.} \ \left[\frac{\partial \mathcal{R}^{\mathrm{U}}(\psi)}{\partial \psi}\right]_{\psi=\psi^{D1}, \psi^{D2}} = 0.$$

Then, we can determine the optimal value of global selfishness $\lambda^\star$ by using $\psi^\star$. Since $||\mathbf{h}_{ji}||^2$ has a Gamma(N_t,2) distribution and there is one-to-one correspondence between ψ and λ, $\lambda^\star$ can be uniquely determined with $\psi^\star$ and derived as

$$\lambda^\star = F^{-1}(1 - \psi^\star; N_t, 2). \tag{20}$$

5.3 Practical cellular network scenario with N_t antennas

We extend our scheme to a general multicell networks. In the previous subsections, we derived our beamforming scheme considering ideal two-cell and practical three-sectored cellular network assuming two transmit antennas. However, it can be easily expended for general N_t antennas system. In the previous subsection, the proposed one-shot beamforming scheme makes each BS nullifies the one of the interference links since we consider that each BS has two transmit antennas. When each BS has $N_\mathrm{t} \geq 3$ transmit antennas, the probability of BS actions are modified. Taking BS_1 as an example, we describe actions of BS_1 and corresponding probabilities in Table 3. Therefore, there are a total of $4^3 = 64$ different cases for three-sectored networks with N_t antennas. Then, we can derive the expectation of sum rate by using probabilities and corresponding sum rate analysis in the same way of Eqs. (13) and (17).

$$\begin{aligned} &\mathbb{E}[\,\mathcal{R}(\psi)] \\ &\leq \psi^6 \log_2 \left(\bar{\Pi}^{(2,2,2)}_{(2,2,2)}\right) + \psi^5 \bar{\psi} \log_2 \left(\bar{\Pi}^{(2,2,1)}_{(2,1,2)} \bar{\Pi}^{(2,2,1)}_{(1,2,2)} \bar{\Pi}^{(2,1,2)}_{(1,2,2)} \bar{\Pi}^{(2,1,2)}_{(2,2,1)} \bar{\Pi}^{(1,2,2)}_{(2,1,2)} \bar{\Pi}^{(1,2,2)}_{(2,2,1)}\right) \\ &\quad + \psi^4 \bar{\psi}^2 \log_2 \left(\bar{\Pi}^{(2,1,1)}_{(2,1,1)} \bar{\Pi}^{(2,1,1)}_{(0,2,2)} \bar{\Pi}^{(2,1,1)}_{(1,2,1)} \bar{\Pi}^{(2,1,1)}_{(1,1,2)} \bar{\Pi}^{(1,2,1)}_{(1,2,1)} \bar{\Pi}^{(1,2,1)}_{(2,0,2)} \bar{\Pi}^{(1,2,1)}_{(2,1,1)} \times \right. \\ &\qquad\qquad \left. \bar{\Pi}^{(1,2,1)}_{(1,1,2)} \bar{\Pi}^{(1,1,2)}_{(1,1,2)} \bar{\Pi}^{(1,1,2)}_{(2,2,0)} \bar{\Pi}^{(1,1,2)}_{(2,1,1)} \bar{\Pi}^{(1,1,2)}_{(1,2,1)} \bar{\Pi}^{(2,2,0)}_{(1,1,2)} \bar{\Pi}^{(2,0,2)}_{(1,2,1)} \bar{\Pi}^{(0,2,2)}_{(2,1,1)}\right) \\ &\quad + \psi^3 \bar{\psi}^3 \log_2 \left(\bar{\Pi}^{(1,1,1)}_{(2,1,0)} \bar{\Pi}^{(1,1,1)}_{(2,0,1)} \bar{\Pi}^{(1,1,1)}_{(1,2,0)} \bar{\Pi}^{(1,1,1)}_{(1,0,2)} \bar{\Pi}^{(1,1,1)}_{(0,1,2)} \bar{\Pi}^{(1,1,1)}_{(0,1,2)} \bar{\Pi}^{(1,1,1)}_{(1,1,1)} \bar{\Pi}^{(1,1,1)}_{(1,1,1)} \times \right. \\ &\qquad\qquad \bar{\Pi}^{(2,1,0)}_{(1,1,1)} \bar{\Pi}^{(2,1,0)}_{(0,1,2)} \bar{\Pi}^{(2,0,1)}_{(1,1,1)} \bar{\Pi}^{(2,0,1)}_{(0,2,1)} \bar{\Pi}^{(1,2,0)}_{(1,1,1)} \bar{\Pi}^{(1,2,0)}_{(1,0,2)} \bar{\Pi}^{(1,0,2)}_{(1,1,1)} \bar{\Pi}^{(1,0,2)}_{(1,2,0)} \times \\ &\qquad\qquad \left. \bar{\Pi}^{(0,1,2)}_{(1,1,1)} \bar{\Pi}^{(0,1,2)}_{(2,1,0)} \bar{\Pi}^{(0,2,1)}_{(1,1,1)} \bar{\Pi}^{(0,2,1)}_{(2,0,1)}\right) \\ &\quad + \psi^2 \bar{\psi}^4 \log_2 \left(\bar{\Pi}^{(1,1,0)}_{(1,1,0)} \bar{\Pi}^{(1,1,0)}_{(0,1,1)} \bar{\Pi}^{(1,1,0)}_{(0,0,2)} \bar{\Pi}^{(1,1,0)}_{(1,0,1)} \bar{\Pi}^{(0,1,1)}_{(0,1,1)} \bar{\Pi}^{(0,1,1)}_{(1,0,1)} \bar{\Pi}^{(0,1,1)}_{(2,0,0)} \times \right. \\ &\qquad\qquad \left. \bar{\Pi}^{(0,1,1)}_{(1,1,0)} \bar{\Pi}^{(1,0,1)}_{(1,0,1)} \bar{\Pi}^{(1,0,1)}_{(0,1,1)} \bar{\Pi}^{(1,0,1)}_{(0,2,0)} \bar{\Pi}^{(1,0,1)}_{(1,1,0)} \bar{\Pi}^{(2,0,0)}_{(0,1,1)} \bar{\Pi}^{(0,2,0)}_{(1,0,1)} \bar{\Pi}^{(0,0,2)}_{(1,1,0)}\right) \\ &\quad + \psi \bar{\psi}^5 \log_2 \left(\bar{\Pi}^{(1,0,0)}_{(0,1,0)} \bar{\Pi}^{(1,0,0)}_{(0,0,1)} \bar{\Pi}^{(0,1,0)}_{(1,0,0)} \bar{\Pi}^{(0,1,0)}_{(0,0,1)} \bar{\Pi}^{(0,0,1)}_{(1,0,0)} \bar{\Pi}^{(0,0,1)}_{(0,1,0)}\right) + \psi^6 \log_2 \left(\bar{\Pi}^{(0,0,0)}_{(0,0,0)}\right) \\ &\equiv \mathcal{R}^{\mathrm{U}}(\psi). \end{aligned} \tag{21}$$

Table 3 BS_1 actions and corresponding probabilities for N_t transmit antennas

Case number	BS_1 action	Probability
Case 1	Egoistic	$\bar{\psi}^2$
Case 2	Altruistic for MS_2	$\bar{\psi}\psi$
Case 3	Altruistic for MS_3	$\bar{\psi}\psi$
Case 4	Altruistic for MS_2 and MS_3	ψ^2

Here, $\mathcal{R}^{\mathrm{U}}(\psi)$ in (21) is an equation of ψ and we can determine the $\psi^\star$ that maximizes $\mathcal{R}^{\mathrm{U}}(\psi)$. Then, we can determine $\lambda^\star$ by using $\psi^\star$. Since $||\mathbf{h}_{ji}||^2$ has a Gamma(N_t,2) distribution and there is one-to-one correspondence between ψ and λ, $\lambda^\star$ can be uniquely determined with $\psi^\star$ and derived as

$$\lambda^\star = F^{-1}(1-\psi^\star; N_t, 2). \tag{22}$$

In this scenario, it is shown that our scheme can be expanded to general N_t antennas scenario though it is not possible to find the closed-form solution for Eq. (22) unlike above two scenarios.

6 Numerical results

We evaluate the performance of the proposed one-shot cooperative beamforming. The average channel gain between the BS in the ith cell and the MS in the jth cell is defined as $E\left[|\mathbf{h}_{ij}|^2\right] = \rho_0 \left(d_{i,j}/d_r\right)^{-\alpha}$, where $d_{i,j}$ denotes the distance between the BS in the ith cell and the MS in the jth cell, and ρ_0 denotes the SNR. The reference distance d_r can be regarded as the cell radius. The values of d_r, the pathloss exponent α are set to 500 m and 3.7, respectively.

Figure 3 shows how the optimal global selfishness $\lambda^\star$ varies with the distance of a MS from a BS, when SNR is 10 and 30 dB. When MS_1 and MS_2 are located from $0.5R$ to R by $0.1R$ interval, where R denotes the cell radius. The results of analysis are computed from the average sum rate approximation while the results of real channel are exhaustively searched from average sum rate observations with real channel realizations. Despite a slight overestimation of $\lambda^\star$, our analysis provides a computationally efficient way to determine $\lambda^\star$. When a MS is located near a BS, the optimal value of λ becomes high, which implies that each cell may act selfishly. As a MS moves toward the cell edge, the optimal value of λ gradually decreases and each cell should act altruistically. Moreover, as we expect, when SNR is 30 dB, the optimal value of λ is less than 10 dB since influence of interference is increased.

In Figs. 4 and 5, we assume an idealized two-cell network scenario and compare the average sum rate performance and cumulative distribution of user rate of the proposed one-shot beamforming scheme with those of conventional cooperative beamforming schemes, i.e., egoistic beamforming (MRT) and altruistic beamforming (ZF), V-SINR based eigen beamforming in [20] and iterative Pareto optimal beamforming in [7]. BSs equip two transmit antennas and MSs equip single antenna. MSs are randomly located in between $0.5R$ and R.

In Fig. 4, the proposed one-shot beamforming outperforms both altruistic and egoistic beamformings in all SNR values. This is because the proposed one-shot

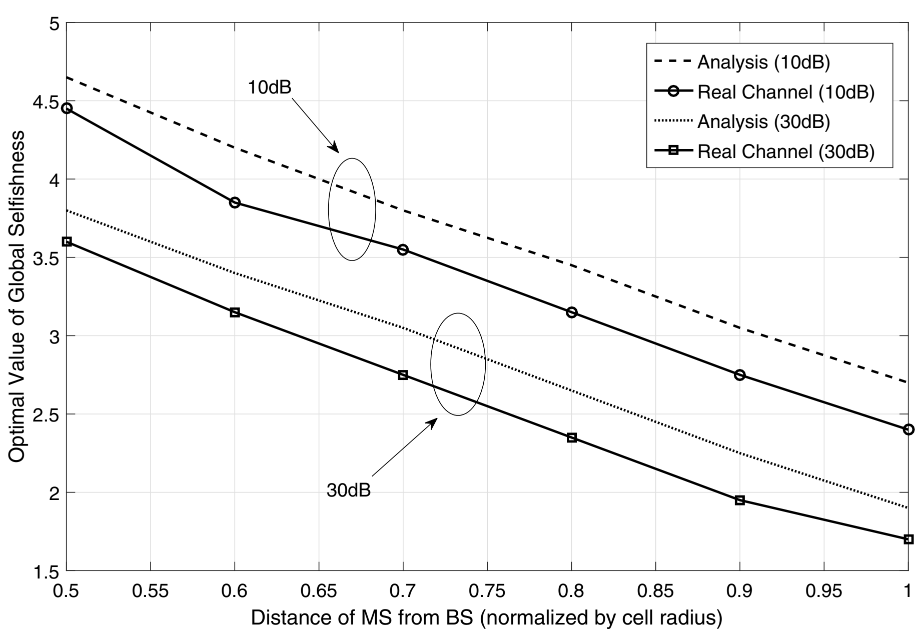

Fig. 3 Optimal global selfishness λ versus distance of MS from BS

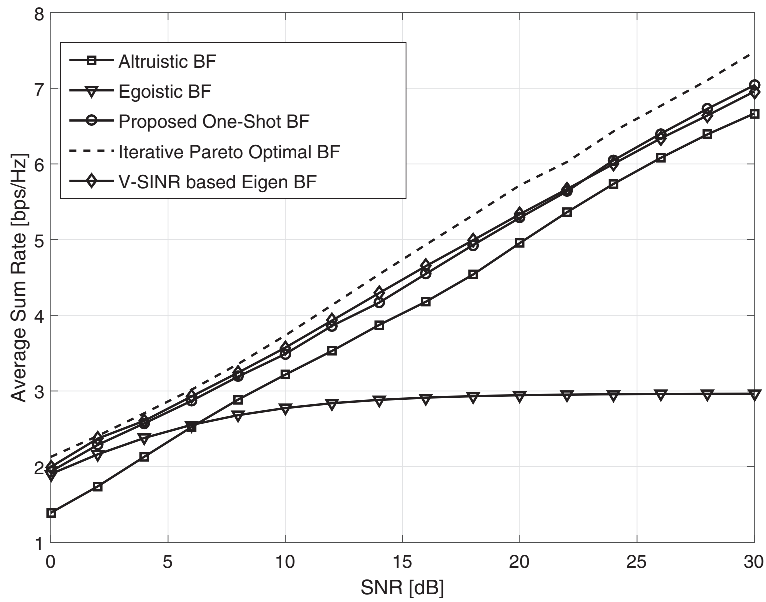

Fig. 4 Average sum rate versus SNR in an ideal two-cell network scenario

beamforming attempts to balance the egoism and altruism with the help of the decision metric, i.e., global selfishness. As compared to V-SINR-based eigen beamforming, our proposed beamforming outperforms V-SINR-based eigen beamforming in high SNR region. The performance of the proposed one-shot beamforming achieves about 95 % of average sum rate performance of the iterative Pareto optimal beamforming. Moreover, the proposed one-shot beamforming offers substantial reduction in computational burden. In Fig. 5, the proposed beamforming scheme outperforms other non-iterative schemes in the performance of cell edge users. As compared to V-SINR-based eigen beamforming, the sum rate performance of the proposed scheme similar to that of V-SINR-based eigen beamforming scheme in average sum rate performance. However, in the performance of cell edge users, the proposed beamforming scheme outperforms V-SINR-based eigen beamforming scheme. This is because V-SINR-based eigen beamforming scheme assumes high SINR unlike the proposed beamforming scheme.

In Figs. 6, 7, 8, and 9, we compare the average sum rate performance and cumulative distribution of user rate

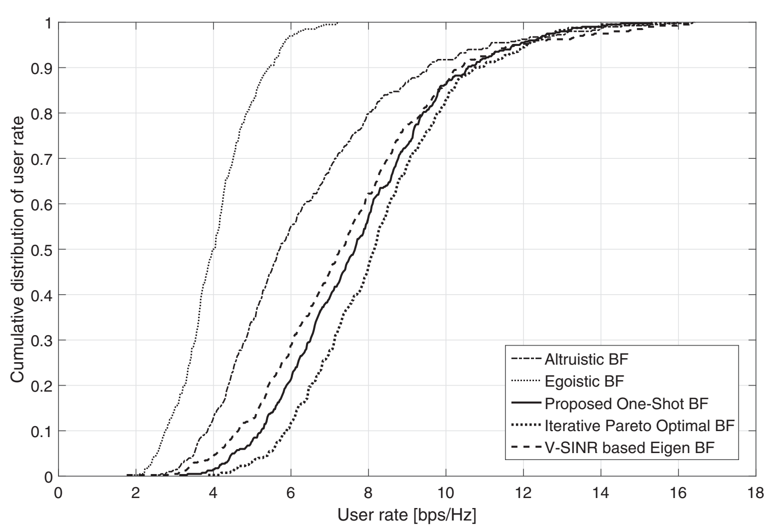

Fig. 5 Cumulative distribution of user rate versus user rate in an ideal two-cell network scenario, when SNR = 30 dB

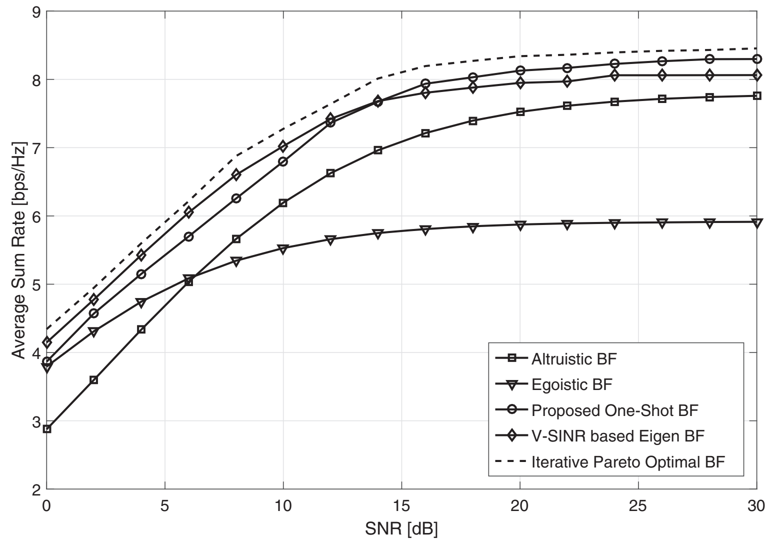

Fig. 6 Average sum rate versus SNR in a practical three-sectored cellular network scenario

in a practical three-sectored network scenario. BSs equip two transmit antennas in Figs. 6 and 7, while BSs equip four transmit antennas in Figs. 8 and 9. MSs equip single antenna and are randomly located in between $0.5R$ and R. The performance of the proposed beamforming is compared to those of egoistic beamforming, altruistic beamforming, V-SINR-based eigen beamforming in [20] and iterative Pareto optimal beamforming in [14]. In Figs. 6 and 8, as already shown in an ideal two-cell network scenario, the proposed one-shot beamforming outperforms both altruistic and egoistic beamformings in all SNR values. As compared to iterative Pareto optimal beamforming in [14], the performances of the proposed one-shot beamforming achieves 96 and 92 % of average sum rate performance of the iterative Pareto optimal beamforming in Figs. 6 and 8, respectively. Moreover, the proposed one-shot beamforming can reduce substantial computational burden since the iterative Pareto optimal beamforming scheme in [14] requires over 70 iterations. Compared to the V-SINR-based eigen beamforming in high SNR region where ICI limits the performance, the proposed one-shot beamforming outperforms the sum rate performances in Figs. 6 and 8 by 8 and 10 %, respectively. The performance improvement of the proposed

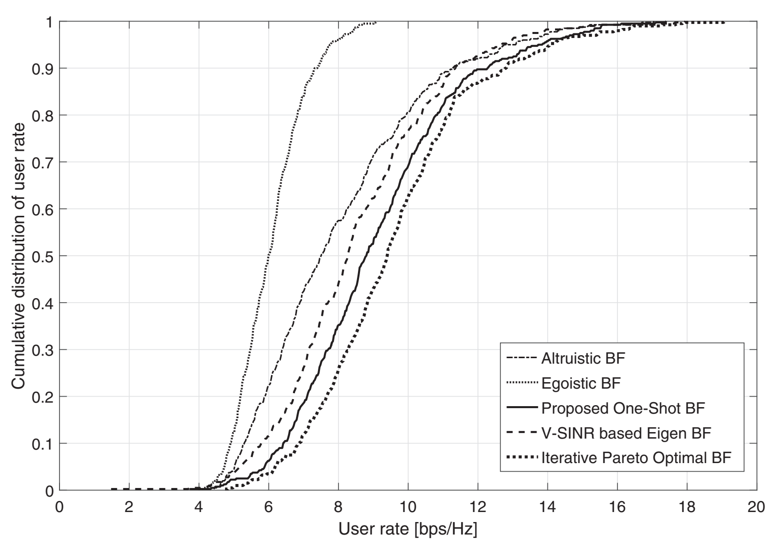

Fig. 7 Cumulative distribution of user rate versus user rate in a practical three-sectored cellular network scenario, when SNR = 30 dB

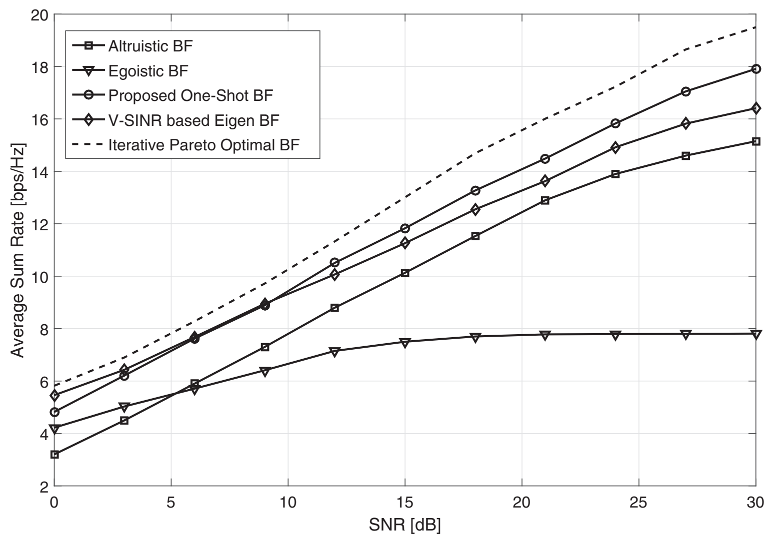

Fig. 8 Average sum rate versus SNR in a practical three-sectored cellular network scenario with $N_t = 4$

one-shot beamforming over V-SINR-based eigen beamforming becomes larger for cell edge users as shown in Figs. 7 and 9. The V-SINR-based eigen beamforming requires some assumptions, e.g., high SINR, which is not required in the proposed beamforming. Moreover, V-SINR-based eigen beamforming scheme aims to maximize sum of V-SINR metric instead of sum rate metric. Whereas, the proposed beamforming focuses on the average sum rate metric to be valid for general $M > 2$ network scenarios. The gap between sum of V-SINR metric and sum rate metric becomes larger in general $M > 2$ cases. Thus, the proposed beamforming scheme can be easily extended to any $M > 2$ network scenarios and outperforms the V-SINR-based eigen beamforming in cell edges and general $M > 2$ network scenarios. This makes our approach more appropriate for practical cellular applications.

7 Conclusions

In this paper, we have proposed a one-shot cooperative beamforming for downlink multicell systems. Unlike conventional non-iterative approaches, we focus the average

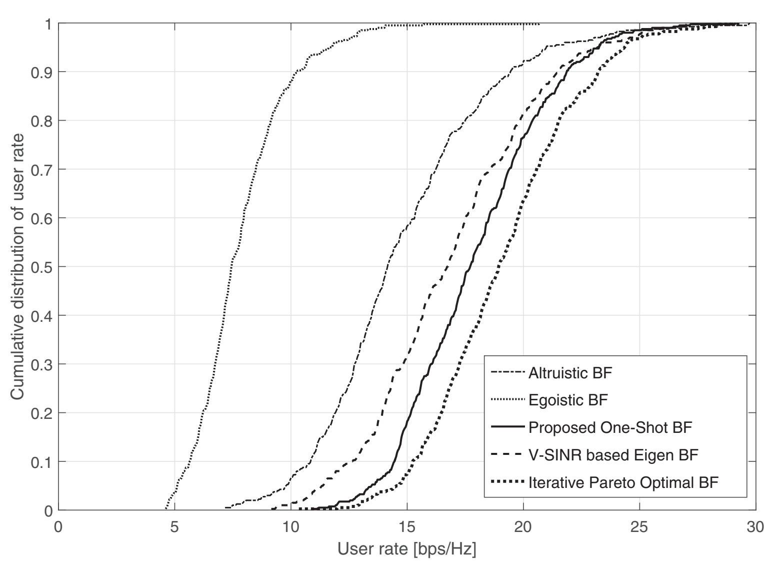

Fig. 9 Cumulative distribution of user rate versus user rate in a practical three-sectored cellular network scenario with $N_t = 4$, when SNR = 30 dB

sum rate metric and determine optimal global selfishness that maximizes sum rate. By using predetermined global selfishness, each BS can autonomously determine whether it behave selfishly or altruistically. The main contributions of this paper are (i) the closed-form derivations of the global selfishness that maximizes average sum rate, (ii) the practical solution for typical three-sectored cellular networks, and (iii) considerable performance improvement especially for cell edge users. Future research direction will include multi-users, multi-antennas at users, heterogeneous networks, etc.

Appendix

Appendix A

There exists two cases for $\Gamma_i^{(e_i,a_i)}$ depending on the choice of interference links nulling. In the first case, the received interference link is nullified by neighboring BS. Therefore, $\Gamma_i^{(e_i,a_i)}$ can be expressed as

$$\Gamma_i^{(e_i,1)} = 1 + \rho_i \chi^2_{2(N_t-e_i)} \quad i = 1, 2. \tag{23}$$

The expectation of Eq. (23) is derived as follows

$$\mathbb{E}\left[\Gamma_i^{(e_i,1)}\right] = 1 + 2\rho_i(N_t - e_i). \tag{24}$$

In the second case, the received interference link is not nullified by other BS and then, $\Gamma_i^{(e_i,a_i)}$ can be expressed as

$$\Gamma_i^{(e_i,0)} = 1 + \frac{\rho_i \chi^2_{2(N_t-e_i)}}{1 + \rho_{ji}\chi^2_2} \quad i,j \in \{1,2\},\ i \neq j. \tag{25}$$

For calculating the expectation of $\Gamma_i^{(e_i,0)}$ in (25), we define random variable $X \equiv \frac{\alpha Z}{1+\beta Y}$, where the random variable $Z \sim \chi^2_{2K}$ and $Y \sim \chi^2_2$. α and β are real-value coefficients. Since Y and Z are independent, the cdf of X can be derived as

$$F_X(x) = 1 - \sum_{n=0}^{K-1}\sum_{l=0}^{n} \frac{\alpha^{l+1-n}}{\beta(n-l)!} \cdot \frac{x^n e^{-x/\alpha}}{(x+\alpha/\beta)^{l+1}}. \tag{26}$$

Then, the expectation of X is derived as follows

$$\begin{aligned}\mathbb{E}[X] &= \int_0^\infty x dF_X = \int_0^\infty 1 - F_X(x)dx \\ &= \sum_{n=0}^{K-1}\sum_{l=0}^{n} \frac{\alpha^{l+1-n}}{\beta(n-l)!} \int_0^\infty \frac{x^n e^{-x/\alpha}}{(x+\alpha/\beta)^{l+1}} dx.\end{aligned} \tag{27}$$

The expression of integral in (27) is derived as

$$\begin{aligned}\int_0^\infty \frac{x^n e^{-x/\alpha}}{(x+\alpha/\beta)^{l+1}} dx = e^{-\beta} \sum_{k=0}^{n} \binom{n}{k} (-\alpha/\beta)^{n-k} \\ \int_{\alpha/\beta}^\infty x^{k-l-1} e^{-x/\alpha} dx.\end{aligned} \tag{28}$$

The integral in (28) can be given as

$$\begin{aligned}R(\alpha,\beta|p) &= \int_{\alpha/\beta}^\infty x^p e^{-x/\alpha} dx \\ &= \begin{cases} e^{-1/\beta} \sum_{i=0}^{p} \frac{p!}{i!} \frac{\alpha^{2i-p-1}}{\beta^i} & \text{if } p \geq 0 \\ E_1(1/\beta) & \text{if } p = -1 \\ \frac{(-\alpha)^{p+1} E_1(1/\beta)}{(-p-1)!} + e^{-1/\beta}\left(\frac{\alpha}{\beta}\right)^{p+1} \sum_{i=0}^{-p-2} \frac{(-p-i-2)!}{(-\beta)^i(-p-1)!} & \text{if } p \leq -2, \end{cases}\end{aligned} \tag{29}$$

where $p = k - l - 1$ and $E_1(\cdot)$ is the first order exponential-integral function.

Appendix B

In Practical three-sectored scenario, there are three cases for $\Gamma_i^{(e_i,a_i)}$ depending on the choice of interference link nulling. In the first case, all the received interference links are nullified by neighboring BSs. In the second case, one interference link is nullified and the other is not nullified. The derivations of the first and the second cases are equal to those of ideal two-cell scenario as derived in Appendix A. In the third case, all the interference links are not nullified by neighboring BSs. Therefore, $\Gamma_i^{(e_i,a_i)}$ can be expressed as

$$\Gamma_i^{(e_i,0)} = 1 + \frac{\rho_i \chi^2_{2(N_t-e_i)}}{1 + \rho_{ji}\chi^2_2 + \rho_{ki}\chi^2_2} \quad i,j,k \in \{1,2,3\},\ i \neq j \neq k. \tag{30}$$

For the calculations of the expectation, we define random variable $X \equiv \frac{\alpha Z}{1+\beta_1 Y_1 + \beta_2 Y_2}$, where the random variable $Z \sim \chi^2_{2K}$, $Y_1 \sim \chi^2_2$ and $Y_2 \sim \chi^2_2$. α, β_1 and β_2 are real-value coefficients. Since the random variables are independent, the cdf of X can be derived as

$$F_X(x) = 1 - \sum_{n=0}^{K-1}\sum_{l=0}^{n} \frac{\alpha^{l+1-n}}{(\beta_1-\beta_2)(n-l)!} \left(\frac{x^n e^{-x/\alpha}}{(x+\alpha/\beta_1)^{l+1}} - \frac{x^n e^{-x/\alpha}}{(x+\alpha/\beta_2)^{l+1}} \right). \tag{31}$$

Then, the expectation of X is derived as

$$\begin{aligned}\mathbb{E}[X] &= \int_0^\infty x dF_X = \int_0^\infty 1 - F_X(x)dx \\ &= \sum_{n=0}^{K-1}\sum_{l=0}^{n} \frac{\alpha^{l+1-n}}{(\beta_1-\beta_2)(n-l)!} \left(\int_0^\infty \frac{x^n e^{-x/\alpha}}{(x+\alpha/\beta_1)^{l+1}} dx - \right. \\ &\qquad \left. \int_0^\infty \frac{x^n e^{-x/\alpha}}{(x+\alpha/\beta_2)^{l+1}} dx \right) \\ &= \sum_{n=0}^{K-1}\sum_{l=0}^{n} \frac{\alpha^{l+1-n}}{(\beta_1-\beta_2)(n-l)!} \left(e^{-\beta_1} \sum_{k=0}^{n} \binom{n}{k} (-\alpha/\beta_1)^{n-k} \cdot R(\alpha,\beta_1|p) \right. \\ &\qquad \left. - e^{-\beta_2} \sum_{k=0}^{n} \binom{n}{k} (-\alpha/\beta_2)^{n-k} \cdot R(\alpha,\beta_2|p) \right)\end{aligned}$$

where $p = k - l - 1$ and $R(\cdot,\cdot|p)$ is the integral expression of (29) in Appendix B.

Acknowledgments
This work was supported by the National Research Foundation of Korea (NRF) grant funded by the Korea government (MSIP) (No. 2014R1A2A2A01003637), and Basic Science Research Program through the National Research Foundation of Korea (NRF) funded by the Ministry of Education (No. NRF-2015R1D1A1A01057100).

Competing interests
The authors declare that they have no competing interests.

Author details
[1]Department of Electrical and Computer Engineering, INMC, Seoul National University, Gwanak-ro, 08826 Seoul, South Korea. [2]Department of Electronic Engineering, Gachon University, Seongnamdae-ro, 13120 Seongnam, South Korea.

Received: 28 November 2015 Accepted: 18 July 2016
Published online: 02 August 2016

References

1. S Catreux, PF Driessen, LJ Greenstein, Simulation results for an interference-limited multiple-input multiple-output cellular system. IEEE Commun. Lett. **4**(11), 334–336 (2000)
2. RS Blum, MIMO capacity with interference. IEEE J. Sel. Areas Commun. **21**(5), 793–801 (2003)
3. 3GPP, coordinated multi-point operation for LTE physical layer aspects (release 11). TR 36.819, v11.1.0, The 3rd Generation Partnership Project (3GPP) (2011)
4. D Gesbert, D Hanly, H Huang, S Shamai, O Simeone, W Yu, Multi-cell MIMO cooperative networks: a new look at interference. IEEE J. Sel. Areas Commun. **28**(9), 1380–1408 (2010)
5. Z-Q Luo, S Zhang, Dynamic spectrum management: complexity and duality. IEEE J. Sel. Topics Signal Process. **2**(1), 57–73 (2008)
6. EG Larsson, EA Jorsweick, Competition versus cooperation on the MISO interference channel. IEEE J. Sel. Areas Commun. **27**(7), 1059–1069 (2008)
7. EA Jorswieck, EG Larsson, D Danev, Complete characterization of the Pareto boundary for the MISO interference channel. IEEE Trans. Signal Process. **56**(10), 5292–5296 (2008)
8. R Zhang, S Cui, Cooperative interference management with MISO beamforming. IEEE Trans. Signal Process. **58**(10), 5454–5462 (2010)
9. X Shang, B Chen, H Poor, Multiuser MISO interference channels with single-user detection: optimality of of beamforming and the achievable rate region. IEEE Trans. Inf. Theory. **57**(7), 4255–4273 (2011)
10. J Lindblom, E Karipidis, EG Larsson, Selfishness and altruism on the MISO interference channel: the case of partial transmit CSI. IEEE Commun. Lett. **13**(9), 667–669 (2009)
11. R Mochaourab, EA Jorswieck, Exchange economy in two-user multiple-input single-output interference channels. IEEE J. Sel. Topics Signal Process. **6**(2), 151–164 (2012)
12. J Lindblom, E Karipidis, in *proceedings of the IEEE European Wireless Conference (EW)*. Cooperative beamforming for the MISO interference channel, (Lucca, 2010)
13. P Cao, EA Jorsweick, S Shi, Pareto Boundary of the rate region for single-stream MIMO interference channels: linear transceiver design. IEEE Trans. Signal Process. **61**(20), 4907–4922 (2013)
14. J Qiu, R Zhang, Z-Q Luo, S Cui, Optimal distributed Beamforming for MISO interference channels. IEEE Trans. Signal Process. **59**(11), 5638–5643 (2011)
15. M Sadek, A Tarighat, AH Sayed, A leakage-based precoding scheme for downlink multi-user MIMO channels. IEEE Trans. Wireless Commun. **6**(5), 1711–1721 (2007)
16. BO Lee, HW Je, O-S Shin, KB Lee, A novel uplink MIMO transmission scheme in a multicell environment. IEEE Trans. Wireless Commun. **8**(10), 4981–4987 (2009)
17. R Zakhour, D Gesbert, in *proceedings of International ITG Workshop on Smart Antennas (WSA)*. Coordination on the MISO interference channel using the virtual SINR framework, (Berlin, 2009)
18. R Zakhour, D Gesbert, Distributed multicell-MISO precoding using the layered virtual SINR framework. IEEE Trans. Wireless Commun. **9**(8), 2444–2448 (2010)
19. R Bhagavatula, R Heath, Adaptive limited feedback for sum rate maximizing beamforming in cooperative multicell systems. IEEE Trans. Signal Process. **59**(2), 800–811 (2011)
20. MA Vazquez, A Perez-Neira, MA Lagunas, Generalized eigenvector for decentralized transmit beamforming in the MISO interference channel. IEEE Trans. Signal Process. **61**(4), 878–882 (2013)
21. N Jindal, JG Andrews, S Weber, in *proceedings of the IEEE International Conference on Communications (ICC)*. Rethinking MIMO for wireless networks: Linear throughput increases with multiple receive antennas, (Dresden, 2009)